Journal of Solid Mechanics Vol. 9, No. 4 (2017) pp. 730-750

Coupled Bending-Longitudinal Vibration of Three Layer Sandwich Beam using Exact Dynamic Stiffness Matrix

A. Zare[1,*] , B. Rafezy [2] ,W.P. Howson [3]

[1]*School of Engineering, Yasouj University, Yasouj, Iran*
[2]*Sahand University of Technology, Tabriz, Iran*
[3] *Independent Consultant, Gwanwyn, Craig Penlline, CF71 7RT, UK*

Received 7 July 2017; accepted 12 September 2017

ABSTRACT

A Newtonian (vectorial) approach is used to develop the governing differential equations of motion for a three layer sandwich beam in which the uniform distribution of mass and stiffness is dealt with exactly. The model allows for each layer of material to be of unequal thickness and the effects of coupled bending and longitudinal motion are accounted for. This results in an eighth order ordinary differential equation whose closed form solution is developed into an exact dynamic member stiffness matrix (exact finite element) for the beam. Such beams can then be assembled to model a variety of structures in the usual manner. However, such a formulation necessitates the solution of a transcendental eigenvalue problem. This is accomplished using the Wittrick-Williams algorithm, whose implementation is discussed in detail. The algorithm enables any desired natural frequency to be converged upon to any required accuracy with the certain knowledge that none have been missed. The accuracy of the method is then confirmed by comparison with five sets of published results together with a further example that indicates its range of application. A number of further issues are considered that arise from the difference between sandwich beams and uniform single material beams, including the accuracy of the characteristic equation, co-ordinate transformations, modal coupling and the application of boundary conditions.

Keywords : Sandwich beam; Exact dynamic stiffness matrix; Coupled motion; Transcendental eigenvalue problem; Wittrick-Williams algorithm.

1 INTRODUCTION

OPTIMISATION of the strength to weight ratio in structural members has been a necessary goal in the aeronautics and space environment for many years and to a lesser extent in many other areas of structural design. Such a philosophy is epitomized by sandwich construction which, in its most usual form, is characterized by a thick lightweight core that is bonded between two thin faceplates of high strength material. An early analysis of the vibrational behavior of sandwich beams was given by Kerwin [1] in the late nineteen fifties and subsequently by a number of authors using a variety of different approaches [2-7], all of which allowed only for transverse inertia. The addition of longitudinal and rotary inertia appears to have been put forward first by Yu [8] in the context of sandwich plate vibration. Later Rao and Nakra [9] also studied these secondary inertia effects in simply supported

*Corresponding author. Tel.: +98 9177073254; Fax: +98 7433221711.
E-mail address: *zare@yu.ac.ir* (M.Zare).

sandwich beams that were unsymmetric about their neutral axis. They showed that there are three families of modes; flexural, extensional and thickness shear and that coupling between them may occur at frequencies of practical interest. Mead [10] confirmed these findings and concluded that the accuracy of the flexural modes thus calculated was superior to earlier theories [3, 5]. Chonan [11] further extended the theory to allow for elastic bonding between the core and face plates. More generally, Mead and Markus [12] showed that coupling between longitudinal and flexural waves was strongest when allowing for both shear deformation and rotational inertia. They concluded that the well-known thickness-shear type of deformation in which the cross-section rotates without translation corresponds to a rotational wave with negligible longitudinal and transverse motion. There have also been some attempts to develop a more accurate way of allowing for shear deformations in the layers by utilizing higher order shear theories [13,14] and the use of variational methods in a variety of forms in order to solve problems with non-classical boundary conditions [13,14,15,16]. Amirani et al [17] extracted the natural frequencies of sandwich beam with functionally graded core using the element free Galerkin method. They used the penalty method for imposition of the essential boundary condition and material discontinuity condition. Hashemi and Adique [18] developed a dynamic finite element method based on the weak integral form of the differential equations of motion governing the free vibration of a symmetric three-layered sandwich beam. Their numerical results showed good agreement with finite element method, exact dynamic stiffness method and other published results. Moreover they also developed a new dynamic finite element model for the free vibration analysis of three-layered sandwich beams applied to an asymmetric steel-face, soft-core sandwich beam, that the face layers follow the Rayleigh beam assumptions, while the core is governed by Timoshenko beam theory and by exploiting only a one-element DFE model [19].

Despite the extensive literature on sandwich beams, there is little work that utilizes a stiffness formulation and also accounts in an exact way for the uniform distribution of mass. Banerjee [20] used an analytical approach to develop the dynamic stiffness matrix for a symmetric three layered beam. His model allowed for axial extension, but assumed that the density of the core material was negligible in comparison to that of the faceplates, which can often be an acceptable simplification, but which inevitably leads to non conservative values of the important lower frequencies. Over the same period, two of the present authors developed an equivalent matrix model for an unsymmetrical three layer sandwich beam that allowed for the density of the core, but ignored the longitudinal inertia [21]. In a later paper, Banerjee and Sobey [22] improved Banerjee's earlier model and allowed for rotary inertia in both the core and the faceplates and additionally allowed for shear deformation of the core material. This is undoubtedly a powerful model, but its complexity will rarely be required in order to analyze the majority of practical applications. Banerjee et al [23] again improved their earlier model for a three-layered sandwich beam of unequal thicknesses which each layer was idealized by the Timoshenko beam theory. They have also used an experimental modal testing set up using the impact hammer kit where the experimental results match reasonably well with theoretical predictions using the dynamic stiffness theory. Jun et al [24] introduced a exact dynamic stiffness method for determining the natural frequencies and mode shapes of laminated composite beams based on third-order shear deformation theory. They also performed a parametric study of the influences of Poisson effect, material anisotropy, slenderness and end condition on the natural frequencies of the composite beam. Khalili et al [25] investigated free vibration of three-layered symmetric sandwich beam using dynamic stiffness and finite element methods. To determine the equations of motion, core density is considered. Natural frequencies were computed using Wittrick–Williams algorithm. They concluded that irrespective of the type of the boundary conditions, increasing the core/face density ratios, decrease the first natural frequency of the sandwich beam, but increasing the face/core thickness ratios and the core shear modulus, increases the first natural frequency of the beam. Damanpack and Khalili [26] investigated high-order free vibration of three-layered symmetric sandwich beam using dynamic stiffness method. They checked the natural frequencies and corresponding vibration modes against those produced by the experiment analysis.

The work of the present paper therefore takes a different course and extends the model of a previous paper [21] to obtain the simplest exact dynamic stiffness model that can be used to analyze practical assemblies of such members realistically. The model is first developed using a vectorial approach that emphasizes the underlying physical relationships that characterize the problem. Attention is then focused on the practical application of the theory. Initially the implementation of the Wittrick-Williams algorithm is considered in detail and leads to a simple description of the fundamental shear thickness mode. This is followed by a discussion on the possible representations of longitudinal displacement and the corresponding implementation of the boundary constraints. Finally guidance is given on a simple way to eliminate the possibility of numerical instability stemming from the characteristic equation.

2 THEORY

The dynamic stiffness matrix of a three layer sandwich beam is now developed from first principles. It accounts exactly for the uniform distribution of mass and stiffness in the member, subject to the following assumptions:

(i) transverse direct strains in the face plates and core are negligible so that small transverse displacements are the same for all points in a normal section;
(ii) there is perfect bonding at the core/faceplate interfaces;
(iii) the face plates are elastic, isotropic and do not deform in shear;
(iv) the linearly elastic core carries only shear and the in-plane normal stresses are assumed to be negligible.

Fig. 1 shows the positive sense of the displacements experienced by a typical section of a sandwich beam at some instant during the motion. The beam has unit width and t_t ,t_c and t_b are the thickness of the top face, core and bottom face, respectively. The face plates are assumed to undergo bending and axial deformation, while the core deforms only in shear. Throughout this text the subscripts *t*, *c*, and *b* refer to the top faceplate, core and bottom faceplate of the three-layered sandwich beam, respectively. Also the generic quantities *m*, *q*, *n* and μ represent bending moment, shear force, axial force and mass/unit length, respectively. When they are not subscripted they are resultant or total values. The prime and dot notations refer to partial differentiation with respect to *x* and time in the usual way.

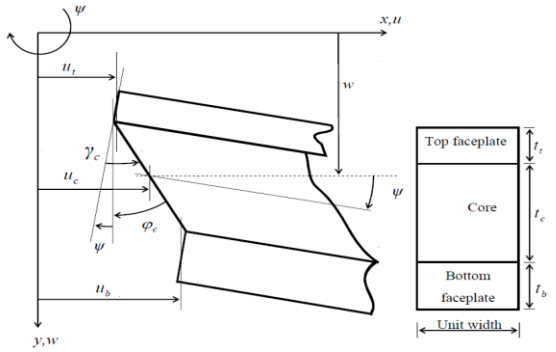

Fig.1
The displaced section, cross-section and co-ordinate system of a typical sandwich beam of unit width.

Due to neglecting transverse direct strains in the face plates and core, small transverse displacements *w* remain constant throughout the section at all layers. Hence, the resultant bending moment at any section is given by

$$m = m_t + m_b = -E_t I_t \psi' - E_b I_b \psi' = -\frac{\psi'}{\kappa} \tag{1a}$$

$$\psi = w' \tag{1b}$$

where $E_i\, I_i$ is the flexural rigidity of face plate i $(i = t, b), \kappa = 1/\left(E_t\, I_t + E_b I_b\right)$ and ψ is the bending slope. It is assumed that plane sections of both the faces and core remain plane as the beam bends. However, in the former they will remain perpendicular to the neutral axis, but not in the latter. Hence, the shear strain in the core layer is given by

$$\gamma_c = \frac{d}{t_c}\left(\psi - \frac{u_t - u_b}{d}\right) \tag{2}$$

where $d = t_c + \frac{t_t + t_b}{2}$ is the distance between centre lines of the face plates and u_t and u_b are the mid-layer longitudinal displacement of the top and bottom faces, respectively. The other necessary force displacement relationships for axial extension and shearing deformation are

$$n_i = E_i t_i \varepsilon_i = E_i t_i u_i' = K_i u' \tag{3a}$$

$$q_c = t_c \tau_c = G_c t_c \gamma_c \tag{3b}$$

where ε_i and $K_i (= E_i t_i)$ are the longitudinal strain and axial rigidity of faceplate i $(i = t, b)$, τ_c and γ_c are the uniform shear stress and strain through the thickness of the core and G_c is the effective shear modulus of the core material. Also it is clear from Fig. 1 that u_c and φ_c, the average longitudinal displacement and rotation of the core, are given by

$$u_c = \frac{u_t + u_b}{2} + \psi e_1 \tag{4a}$$

$$\varphi_c = \frac{u_t - u_b - \psi e_2}{t_c} \tag{4b}$$

respectively, where $e_1 = \frac{t_b - t_t}{4}$ and $e_2 = \frac{t_b + t_t}{2}$.

Now consider Fig. 2, which shows the forces acting on a typical elemental length of a member at some instant during the motion. The equation of horizontal equilibrium can then be written as:

$$\frac{\partial n_t}{\partial x} + \frac{\partial n_b}{\partial x} = \mu_t \ddot{u}_t + \mu_c \ddot{u}_c + \mu_b \ddot{u}_b \tag{5}$$

Substituting Eqs. (4a) and (3a) into Eq. (5) gives the first differential equation of motion as:

$$K_t u_t'' + K_b u_b'' - (\mu_t + \frac{\mu_c}{2})\ddot{u}_t - (\mu_b + \frac{\mu_c}{2})\ddot{u}_b - \mu_c e_1 \ddot{\psi} = 0 \tag{6}$$

In similar fashion, the equation of vertical equilibrium is

$$\frac{\partial q}{\partial x} = \mu \ddot{w} \tag{7}$$

Comparing Figs. 2 and 3 and using Eq. (3b), it is clear that $q = q_t + q_b + q_c$ is the resultant shear force at any normal section of the element. Thus taking moments about the centre line at the right hand side of the bottom faceplate in Fig.2 and ignoring terms of second order yields the moment equilibrium equation as

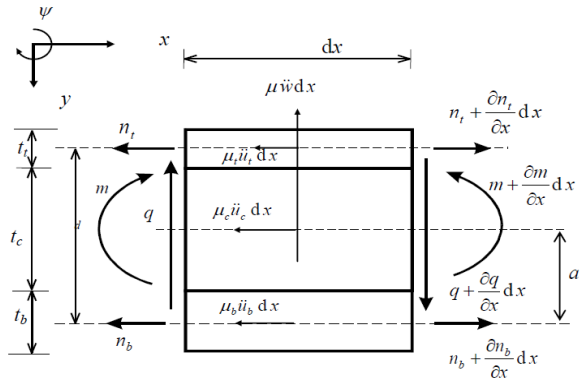

Fig.2
Positive resultant forces, moments and reversed linear inertias acting on a typical elemental length of a sandwich beam of unit width in local co-ordinates. The layer dimensions are also shown.

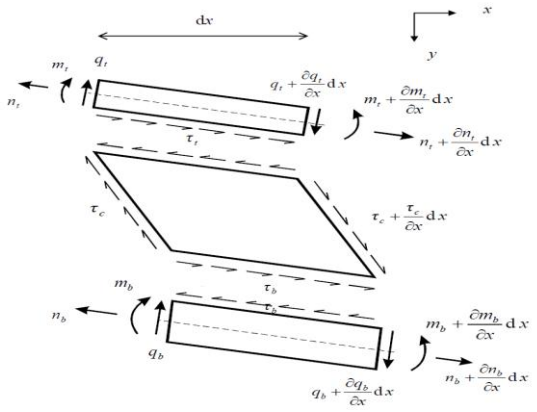

Fig.3
Component member forces, moments and inter-member stresses on a typical elemental length of a sandwich beam.

$$q\,\mathrm{d}x - \frac{\partial m}{\partial x}\mathrm{d}x + \frac{\partial n_t}{\partial x}\mathrm{d}x\,(d) - \mu_t \ddot{u}_t\,\mathrm{d}x\,(d) - \mu_c \ddot{u}_c\,\mathrm{d}x\,(a) = 0 \tag{8}$$

where $d = t_c + \dfrac{t_t + t_b}{2}$ is the distance between the centre lines of the two faceplate and the core and m is the resultant bending moment at any section given by Eq. (1a). Substituting Eqs. (1a), (3a) and (4a) into Eq. (8) yields the resultant shear force as:

$$q = -\frac{\psi''}{\kappa} - K_t d\,u_t'' + (d\mu_t + a\frac{\mu_c}{2})\ddot{u}_t' + a\frac{\mu_c}{2}\ddot{u}_b' + ae_1\mu_c\ddot{\psi} \tag{9}$$

Differentiating and substituting Eq. (9) into Eq. (7) gives the second differential equation of motion as:

$$\mu\ddot{w}' + \frac{\psi'''}{\kappa} + K_t d\,u_t''' - (d\mu_t + a\frac{\mu_c}{2})\ddot{u}_t'' - a\frac{\mu_c}{2}\ddot{u}_b'' - ae_1\mu_c\ddot{\psi}'' = 0 \tag{10}$$

Consider finally the horizontal equilibrium of the top faceplate in Fig. 3, which may be written as:

$$\frac{\partial n_t}{\partial x}\mathrm{d}x + \tau_t\,\mathrm{d}x = \mu_t\frac{\partial^2 u_t}{\partial t^2}\mathrm{d}x \tag{11}$$

where τ_t is the shear stress at the interface between the top faceplate and the core. It then follows that

$$\tau_t = -K_t u_t'' + \mu_t\ddot{u}_t \tag{12}$$

In addition, the equation of horizontal equilibrium of the bottom faceplate in Fig. 3 may be written as:

$$\frac{\partial n_b}{\partial x}\mathrm{d}x - \tau_b\,\mathrm{d}x = \mu_b\frac{\partial^2 u_b}{\partial t^2}\mathrm{d}x \tag{13}$$

where τ_b is the shear stress at the interface between the bottom faceplate and the core. Hence

$$\tau_b = K_b u_b'' - \mu_b\ddot{u}_b \tag{14}$$

Since it was assumed that the shear stress through the core thickness has an average value of τ_c, the equation of moment equilibrium of the core about the midpoint of the right hand side of the core in Fig. 3 can be written as:

$$-\tau_t \,\mathrm{d}x\,\frac{t_c}{2}-\tau_b \,\mathrm{d}x\,\frac{t_c}{2}+\tau_c t_c \,\mathrm{d}x=0 \tag{15}$$

Substituting Eqs. (2), (3b), (12) and (14) into Eq. (15) yields the last differential equation of motion as:

$$K_t u_t''-\mu_t \ddot{u}_t-K_b u_b''+\mu_b \ddot{u}_b+\frac{2G_c d}{t_c}\psi-\frac{2G_c}{t_c}u_t+\frac{2G_c}{t_c}u_b=0 \tag{16}$$

Attention is now confined to harmonic motion in which the time dependent terms are related to ω, the circular frequency, by the generic equation

$$f(x,t)=F(x)\,e^{\mathrm{i}\omega t} \tag{17}$$

where the upper case character refers to the amplitude of the equivalent time dependent quantity. Hence, using the appropriate form of Eq. (17) in the partial differential Eqs. (10), (6) and (16) yields the following linear differential equations with constant coefficients

$$\left.\begin{aligned}
&-\mu\omega^2 W+\frac{W''''}{\kappa}+K_t d\,U_t'''+(d\mu_t+a\frac{\mu_c}{2})\omega^2 U_t'+a\frac{\mu_c}{2}\omega^2 U_b'+ae_1\mu_c\omega^2 W''=0\\
&K_t U_t''+K_b U_b''+(\mu_t+\frac{\mu_c}{2})\omega^2 U_t+(\mu_b+\frac{\mu_c}{2})\omega^2 U_b+\mu_c e_1\omega^2 W'=0\\
&K_t U_t''+\mu_t\omega^2 U_t-K_b U_b''-\mu_b\omega^2 U_b+\frac{2G_c d}{t_c}W'-\frac{2G_c}{t_c}U_t+\frac{2G_c}{t_c}U_b=0
\end{aligned}\right\} \tag{18}$$

Rewriting Eqs. (18) in matrix form and introducing the operator $D=\mathrm{d}/\mathrm{d}x$,

$$\begin{bmatrix}
\frac{D^4}{\kappa}+ae_1\mu_c\omega^2D^2-\mu\omega^2 & K_t d\,D^3+(d\mu_t+a\frac{\mu_c}{2})\omega^2 D & a\frac{\mu_c}{2}\omega^2 D\\
\mu_c e_1\omega^2 D & K_t D^2+(\mu_t+\frac{\mu_c}{2})\omega^2 & K_b D^2+(\mu_b+\frac{\mu_c}{2})\omega^2\\
\frac{2G_c d}{t_c}D & K_t D^2+\mu_t\omega^2-\frac{2G_c}{t_c} & -K_b D^2-\mu_b\omega^2+\frac{2G_c}{t_c}
\end{bmatrix}\begin{bmatrix}W\\U_t\\U_b\end{bmatrix}=0 \tag{19}$$

Eqs. (19) can be rewritten in symmetric form using the following operations that do not alter its determinant.

i) Add the last two rows of Eq. (19) and divide by 2 to give the second row of Eq. (20).
ii) Subtract the third row of Eq. (19) from the second row and divide by 2 to give the third row of Eq. (20).
iii) Finally, differentiate the second row of Eq. (20) once, multiply by *d* and then subtract it from the first row of Eq. (19) to give the first row of Eq. (20).

These operations yield

$$\begin{bmatrix}
A_1D^4+A_2D^2+A_3 & (A_4+A_5)D & (-A_4+A_5)D\\
(A_4+A_5)D & A_6D^2+A_7 & A_8\\
(-A_4+A_5)D & A_8 & A_9D^2+A_{10}
\end{bmatrix}\begin{bmatrix}W\\U_t\\U_b\end{bmatrix}=0 \tag{20}$$

where

$$\left.\begin{aligned}
&A_1=1/\kappa;\quad A_2=-\hat{S}_c+\mu_c e_1^2\omega^2;\quad A_3=-\mu\omega^2;\quad A_4=\hat{S}_c/d;\\
&A_5=\frac{\mu_c}{2}e_1\omega^2;\quad A_6=K_t;\quad A_7=(\mu_t+\mu_c/4)\omega^2-\hat{S}_c/d^2;\\
&A_8=\hat{S}_c/d^2+\omega^2\mu_c/4;\quad A_9=K_b;\quad A_{10}=(\mu_b+\mu_c/4)\omega^2-\hat{S}_c/d^2
\end{aligned}\right\} \tag{21}$$

and $\hat{S}_c = \dfrac{G_c d^2}{t_c}$.

It is interesting to note that all component parts of the $A_i\,(i=1,...,10)$ that contain ω^2 stem from the inclusion of coupled longitudinal inertia, except for term A_3.

Eqs. (19) or (20) can now be used to develop the eighth order differential equation governing the motion of the beam by eliminating all but one of W, U_t or U_b to give

$$[D^8 + c_1 D^6 + c_2 D^4 + c_3 D^2 + c_4]V = 0 \tag{22}$$

where $V = W$, U_t or U_b;

$$\left.\begin{aligned}
c_1 &= (\frac{1}{\hat{\varsigma}} + \frac{\mu_c}{4\varsigma} + \mu_c \kappa\ e_1^2)\omega^2 - \hat{S}_c(\frac{1}{d^2\varsigma} + \kappa\ ) \\
c_2 &= (\frac{\mu_t \mu_b}{K_t K_b} + \frac{\mu_c(\mu_1+\mu_2)}{4K_t K_b} + \frac{\mu_c \kappa\, e_1^2}{\hat{\varsigma}})\omega^4 + [\frac{\hat{S}_c \mu_c \kappa\, e_1}{\varsigma d}\ (\frac{K_t - K_b}{K_t + K_b} - \frac{e_1}{d}\ ) - \hat{S}_c \kappa(\frac{1}{\hat{\varsigma}} + \frac{\mu_c}{4\varsigma}) - \mu(\kappa + \frac{\hat{S}_c}{d^2 K_t K_b})]\omega^2 \\
c_3 &= [\frac{\mu_c \mu_t \mu_b \kappa\, e_1^2}{K_t K_b}\ ]\omega^6 - \{\mu\,\kappa\ (\frac{1}{\hat{\varsigma}} + \frac{\mu_c}{4\varsigma}) + \frac{\hat{S}_c \kappa}{K_t K_b}[\mu_t \mu_b + \frac{\mu_c\ e_1}{d}(\mu_b - \mu_t) + \mu_c(\mu_t + \mu_b)(\frac{1}{4} + \frac{e_1^2}{d^2}\ )]\}\omega^4 + \frac{\hat{S}_c \mu\,\kappa}{\varsigma d^2}\omega^2 \\
c_4 &= -[\frac{\mu_t \mu_b}{K_t K_b} + \frac{\mu_c(\mu_t + \mu_b)}{4K_t K_b}]\mu\,\kappa\,\omega^6 + \frac{\hat{S}_c \mu^2 \kappa}{d^2 K_t K_b}\omega^4
\end{aligned}\right\} \tag{23}$$

and

$$\varsigma = K_t K_b / (K_t + K_b);\quad \hat{\varsigma} = K_t K_b / (K_t \mu_t + K_b \mu_b). \tag{24}$$

Expressions for the general displacements W, Ψ, U_t and U_b can now be deduced using Eqs. (1b), (17) and (22), while expressions for the corresponding forces can be obtained by imposing Eq. (17) on Eqs. (9), (1a) and (3a) to yield

$$\left.\begin{aligned}
Q &= -\frac{W'''}{\kappa} - a e_1 \mu_c \omega^2 W' - K_t d\, U_t'' - (\mu_t d + \mu_c \frac{a}{2})\omega^2 U_t - \mu_c \frac{a}{2}\omega^2 U_b \\
M &= -\frac{W''}{\kappa} \\
N_t &= K_t U_t' \\
N_b &= K_b U_b'
\end{aligned}\right\} \tag{25}$$

We now seek to solve the governing differential equation of motion, Eq. (22), for the harmonically varying displacement field. Eq. (22) is a linear differential equation with constant coefficients and its solution can be sought in the following form

$$V = \sum_{j=1}^{8} \bar{C}_{ij} \zeta_j \qquad (i = 1,2,...8) \tag{26a}$$

where

$$\zeta_j = e^{\eta_j x};\quad 0 < x < L \tag{26b}$$

The $\bar{C}_{ij}$ $(i = 1,2,...8)$ are arbitrary constants and η_j $(j = 1,8)$ are the roots of the characteristic equation stemming from Eq. (22), i.e. the roots of

$$\eta^8 + c_1\eta^6 + c_2\eta^4 + c_3\eta^2 + c_4 = 0 \tag{27}$$

The η_j define V (W, U_t or U_b) and the other necessary quantities for the stiffness formulation of the problem, i.e. Eqs. (1b) and (25) to yield the following results

$$\left.\begin{aligned} W &= \sum_{j=1}^{8} H_{1j} C_j \zeta_j \quad Q = \sum_{j=1}^{8} H_{5j} C_j \zeta_j \\ \Psi &= \sum_{j=1}^{8} H_{2j} C_j \zeta_j \quad M = \sum_{j=1}^{8} H_{6j} C_j \zeta_j \\ U_t &= \sum_{j=1}^{8} H_{3j} C_j \zeta_j \quad N_t = \sum_{j=1}^{8} H_{7j} C_j \zeta_j \\ U_b &= \sum_{j=1}^{8} H_{4j} C_j \zeta_j \quad N_b = \sum_{j=1}^{8} H_{8j} C_j \zeta_j \end{aligned}\right\} \tag{28}$$

where $H_{ij} C_j = \bar{C}_{ij}$, such that C_j is common to all the equations and H_{ij} is the relational constant. Noting that one of the H_{ij} is arbitrary, it is convenient to set $H_{1j} = 1$. This, together with the use of Eqs. (21), yields the following relationships between the H_{ij} of Eqs. (28)

$$\left.\begin{aligned} &H_{1j} = 1 \qquad H_{2j} = \eta_j \qquad H_{3j} = \frac{A_8(A_1\eta_j^4 + A_2\eta_j^2 + A_3) - (A_5^2 - A_4^2)\eta_j^2}{[(A_6\eta_j^2 + A_7)(A_5 - A_4) - A_8(A_4 + A_5)]\eta_j} \\ &H_{4j} = -\frac{(A_4 + A_5)\eta_j + (A_6\eta_j^2 + A_7)H_{3j}}{A_8} \\ &H_{5j} = -\{\frac{\eta_j^3}{\kappa} + ae_1\mu_c\omega^2\eta_j + [K_t d\,\eta_j^2 + (\mu_t d + \mu_c\frac{a}{2})\omega^2]H_{3j} + \mu_c\frac{a}{2}\omega^2 H_{4j}\} \\ &H_{6j} = -\eta_j^2/\kappa \qquad H_{7j} = K_t\eta_j H_{3j} \qquad H_{8j} = K_b\eta_j H_{4j} \end{aligned}\right\} \tag{29}$$

It is now convenient to switch from the local co-ordinate system of Fig. 4(a) to the member co-ordinate system of Fig. 4(b). Comparison of the two figures shows that this is equivalent to imposing the conditions of Eqs. (30) onto Eqs. (28).

$$\begin{aligned} &\text{At } x = 0: \; W = W_1,\; \Psi = \Psi_1,\; U_t = U_{t1},\; U_b = U_{b1},\; Q = -Q_1,\; M = M_1,\; N_t = -N_{t1},\; N_b = -N_{b1} \\ &\text{At } x = L: \; W = W_2,\; \Psi = \Psi_2,\; U_t = U_{t2},\; U_b = U_{b1},\; Q = Q_2,\; M = -M_2,\; N_t = N_{t2},\; N_b = N_{b2} \end{aligned} \tag{30}$$

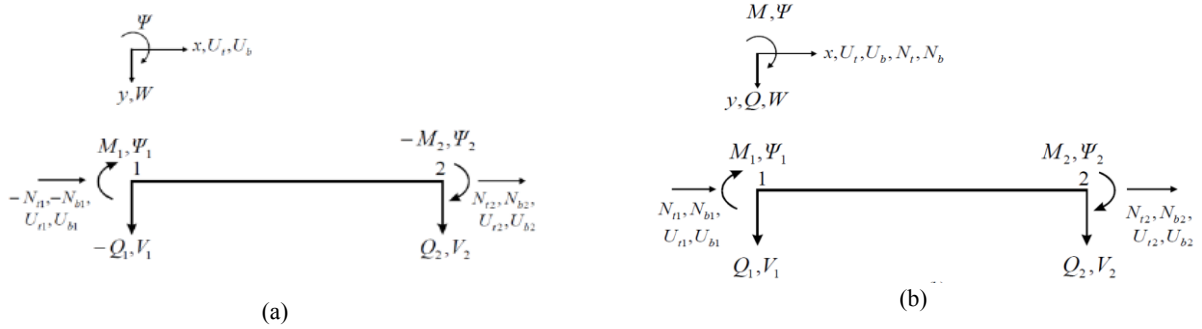

Fig.4
Nodal forces and displacements of a sandwich beam a) in local coordinates, b) in member coordinates.

The resulting matrix equations are given by

$$\mathbf{d} = \mathbf{S}\,\mathbf{C} \tag{31a}$$

and

$$\mathbf{p} = \mathbf{S}^{*}\mathbf{C} \tag{31b}$$

where

$$\mathbf{d} = \begin{bmatrix} W_1 \\ \Psi_1 \\ U_{t1} \\ U_{b1} \\ W_2 \\ \Psi_2 \\ U_{t2} \\ U_{b2} \end{bmatrix}, \quad \mathbf{p} = \begin{bmatrix} Q_1 \\ M_1 \\ N_{t1} \\ N_{b1} \\ Q_2 \\ M_2 \\ N_{t2} \\ N_{b2} \end{bmatrix}, \quad \mathbf{C} = \begin{bmatrix} C_1 \\ C_2 \\ C_3 \\ C_4 \\ C_5 \\ C_6 \\ C_7 \\ C_8 \end{bmatrix} \tag{32}$$

and

$$\left.\begin{array}{l} s_{1j} = H_{1j} \quad ; s_{2j} = H_{2j} \quad ; s_{3j} = H_{3j} \quad ; s_{4j} = H_{4j} \\ s_{5j} = H_{1j}\,\chi_j \; ; s_{6j} = H_{2j}\,\chi_j \; ; s_{7j} = H_{3j}\,\chi_j \; ; s_{8j} = H_{4j}\,\chi_j \\ \\ s^{*}_{1j} = -H_{5j} \quad ; s^{*}_{2j} = H_{6j} \quad ; s^{*}_{3j} = -H_{7j} \quad ; s^{*}_{4j} = -H_{8j} \\ s^{*}_{5j} = H_{5j}\,\chi_j \; ; s^{*}_{6j} = -H_{6j}\,\chi_j \; ; s^{*}_{7j} = H_{7j}\,\chi_j \; ; s^{*}_{8j} = H_{8j}\,\chi_j \\ \\ \chi_j = e^{\eta_j} \end{array}\right\} \quad (j = 1,2,\ldots 8) \tag{33}$$

where s_{ij} and s^{*}_{ij} are the elements of **S** and **S***, respectively, and their subscripts correspond to row and column co-ordinates in the usual way. The required dynamic stiffness matrix, ***k***, follows from Eq. (31) through the following steps. From Eq. (31a),

$$\mathbf{C} = \mathbf{S}^{-1}\ \mathbf{d} \tag{34}$$

and substituting in Eq. (31b) gives

$$\mathbf{p} = \mathbf{k}\ \mathbf{d} \tag{35}$$

where

$$\mathbf{k} = \mathbf{S}^{*}\ \mathbf{S}^{-1} \tag{36}$$

The dynamic stiffness matrix for the overall structure can now be assembled from the element matrices in the usual way. The use of 'exact' finite elements leads to an idealization containing the minimum number of elements, while leaving invariant the accuracy to which any particular natural frequency can be converged upon. This can be important for higher natural frequencies and should be contrasted with traditional finite elements in which the accuracy is sensitive to the idealization. Once the required natural frequencies have been determined, the corresponding mode shapes can be retrieved by any reliable method. The method for converging with certainty on the required natural frequencies is now described.

3 WITTRICK-WILLIAMS ALGORITHM

The Wittrick-Williams algorithm [27], has been available for over forty years and states that

$$J = J_0 + s\{\mathbf{K}\} \tag{37}$$

where J is the number of natural frequencies of the structure exceeded by some trial frequency, ω^*, J_0 is the number of natural frequencies which would still be exceeded if all the elements were clamped at their ends so as to make $\mathbf{D} = \mathbf{0}$, and $s\{\mathbf{K}\}$ is the sign count of the matrix $\mathbf{K}$. $s\{\mathbf{K}\}$ is defined in reference [27] and is equal to the number of negative elements on the leading diagonal of the upper triangular matrix obtained from $\mathbf{K}$, when $\omega = \omega^*$, by the standard form of Gauss elimination without row interchanges. A knowledge of J corresponding to any trial frequency makes it possible to develop a method for converging upon any required natural frequency to any desired accuracy. However, while $s\{\mathbf{K}\}$ is easily computed, the value of J_0 is more difficult to determine and is dealt with below.

From the definition of J_0 it can be seen that

$$J_0 = \sum J_m \tag{38}$$

where J_m is the number of natural frequencies of a component member, with its ends clamped, which have been exceeded by ω^*, and the summation extends over all such members. In some cases it is possible to determine the value of J_m for the element type symbolically, using a direct approach. However, this is impractical in the present case due to the algebraic complexity of the expressions. Instead, the same result is achieved by an argument based on Eq. (37) that was originally put forward by Howson and Williams [28].

Consider a component member that has been isolated from the remainder of the structure by clamping its ends. Treating this member as a complete structure, it is evident that the required value of J_m could be evaluated if its natural frequencies were known. Unfortunately, this simple structure can rarely be solved easily. We therefore seek to establish a different set of boundary conditions that admit a simple symbolic solution and which enable solutions to the clamped ended case to be deduced. This is most easily achieved by imposing roller-roller supports which, in this case, permit rotation and longitudinal motion of the faceplates, i.e. Ψ, U_t and U_b respectively, but prevent lateral displacement W, see Fig. 5.

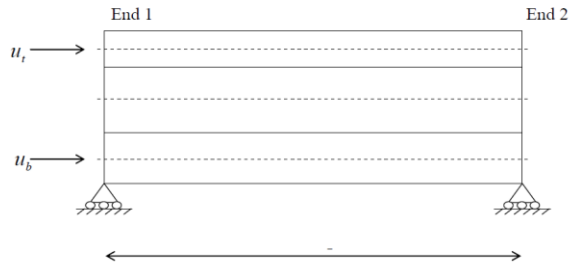

Fig.5
Roller-roller supported beam and the position of axial freedoms through the beam thickness.

Let the stiffness matrix for this structure be $\mathbf{k}^{rr}$, then the number of roots exceeded by ω^* is given by Eq. (37) and the arguments above as:

$$J_{rr} = J_m + s\{\mathbf{k}^{rr}\} \tag{39}$$

where J_{rr} is the number of natural frequencies that lie below the trial frequency for the member with roller-roller supports. It then follows directly that

$$J_m = J_{rr} - s\{\mathbf{k}^{rr}\} \tag{40}$$

Once more $\mathbf{k}^{rr}$, and hence $s\{\mathbf{k}^{rr}\}$, is readily obtained, this time from Eq. (35). J_{rr} is slightly more difficult, but relates to the element with boundary conditions that yield a simple exact solution, as shown below.

For the roller-roller-supported case, the boundary conditions are defined by

$$N_{t1} = N_{t2} = N_{b1} = N_{b2} = M_1 = M_2 = W_1 = W_2 = 0 \tag{41}$$

Now it can be seen from Eq. (25) that N_{ti} and N_{bi}, the amplitude of the axial forces in the top and bottom faceplates, are functions of U_i' $(i = t \text{ and } b)$. These conditions are therefore satisfied by assuming solutions of the form

$$W = B_1 \sin \delta x \qquad U_t = B_2 \cos \delta x \qquad U_b = B_3 \cos \delta x \tag{42}$$

where B_1, B_2 and B_3 are constants and $\delta = \dfrac{n\pi}{L}$ $(n = 0,1,2,3,\ldots)$. Since Eq. (22) is a combined equation that allows for the effects of W, U_t and U_b, substituting any part of Eq. (42) into Eq. (22) yields

$$\delta^8 - c_1\delta^6 + c_2\delta^4 - c_3\delta^2 + c_4 = 0 \tag{43}$$

A further substitution of Eqs.(23) into Eq. (43) leads to the following frequency equation for a roller-roller supported beam

$$b_1\omega^6 + b_2\omega^4 + b_3\omega^2 + b_4 = 0 \tag{44}$$

where

$$\left.\begin{aligned}
b_1 &= -\frac{\kappa}{K_t K_b}[\mu_t\mu_b(\mu + \delta^2\mu_c e_1^2) + \mu\,\mu_c(\mu_t + \mu_b)/4] \\
b_2 &= \frac{\hat{S}_c\mu^2\kappa}{d^2K_tK_b} + [\frac{\hat{S}_c\kappa}{K_tK_b}\{\mu_t\mu_b + \frac{\mu_c\, e_1}{d}(\mu_b - \mu_t) + \mu_c(\mu_t + \mu_b)\,(\frac{1}{4} + \frac{e_1^2}{d^2})\} \\
&\qquad + \mu\,\kappa\,(\frac{1}{\hat{\varsigma}} + \frac{\mu_c}{4\varsigma})\,]\delta^2 + (\frac{\mu_t\mu_b}{K_tK_b} + \frac{\mu_c(\mu_t + \mu_b)}{4K_tK_b} + \frac{\mu_c\kappa\, e_1^2}{\hat{\varsigma}})\delta^4 \\
b_3 &= -\frac{\hat{S}_c\mu\,\kappa}{\varsigma\, d^2}\,\delta^2 + [\frac{\hat{S}_c\mu_c\kappa\, e_1}{\varsigma\, d}(\frac{K_t - K_b}{K_t + K_b} - \frac{e_1}{d}) - \hat{S}_c\kappa\,(\frac{1}{\hat{\varsigma}} + \frac{\mu_c}{4\varsigma}) - \mu\,(\kappa + \frac{\hat{S}_c}{d^2K_tK_b})]\delta^4 - (\frac{1}{\hat{\varsigma}} + \frac{\mu_c}{4\varsigma} + \mu_c\kappa\, e_1^2)\delta^6 \\
b_4 &= \hat{S}_c(\frac{1}{d^2\varsigma} + \kappa\,)\,\delta^6 + \delta^8
\end{aligned}\right\} \tag{45}$$

Eq. (44) can be expressed as a cubic equation in ω^2 and consequently its real, positive roots are the square of its natural frequencies for each value of n = 0,1,2, …. Hence J_{rr} is given by the number of positive values of ω_n that lie below the trial frequency, ω^*. Thus, substituting Eq. (40) in to Eq. (38) gives

$$J_0 = \sum(J_{rr} - s\,\{\mathbf{k}^{rr}\}) \tag{46}$$

The required value of J then follows from Eq. (37). It is interesting to note that when $n = 0, \delta = 0$ and the coefficients b_3 and b_4 are zero. For this case it can be shown that b_1 is always negative and that b_2 is always positive.

Eq. (44) then yields a single non-trivial real root. It is equally clear from Eq. (42) that

$$V = 0 \ ; \ U_t = B_2 \ ; \ U_b = B_3 \tag{47}$$

Thus the mode corresponding to $n = 0$ has no lateral displacement and rigid body displacements horizontally. Thus there is no axial extension and the frequency corresponds to the fundamental shear thickness mode.

4 TRANSFORMATION MATRICES

The stiffness matrix formulation of a sandwich beam, using the sign convention of Fig. 1 and including the effects of both transverse and longitudinal inertia, leads to the set of boundary conditions stated in Eqs. (30). However, it is possible to formulate the problem via a number of possible sets of displacement variables together with their corresponding sets of boundary conditions. For example, rather than using the mid-layer displacement of the faceplates as being representative of the longitudinal displacement, u_t and u_b in Fig. 6, the displacements at the interface of the core and the faceplates, u_2 and u_3, or the longitudinal displacements at the external fibers of the faceplates, u_1 and u_4, could equally well be used. However, in contrast to conventional homogeneous beams, these alternative sets of axial displacements, which also correspond to possible locations of axial constraint, can significantly influence the natural frequencies [29]. Fortunately, the dynamic stiffness matrix of Eq. (35) can be made to be compatible with any required set of field displacements by appropriate transformation. Once the desired configuration has been achieved, it can be used to model general two dimensional structures by further transformation from local to global co-ordinates see Fig.7. Details of all these transformations are given in the Appendix.

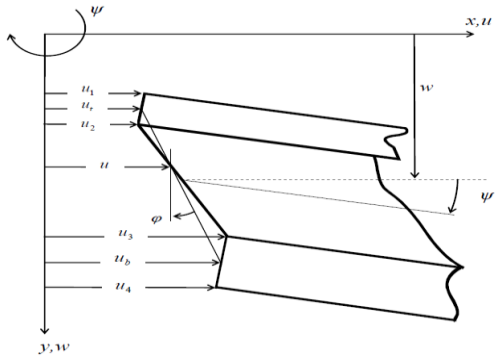

Fig.6
The displaced section showing the possible displacement field variables (u_i) of a typical sandwich beam section of unit width. Note that the vertical position of the longitudinal displacement *u* is not a geometric property of the section, but a function of u_t and u_b.

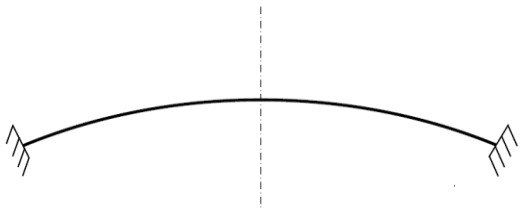

Fig.7
Clamped-clamped curved sandwich beam of Example 4. The length of the beam is 0.7112*m* and its radius is 4.2672*m*.

This figure ignored in uncorrected proof version of the paper.

5 NUMERICAL RESULTS

A number of examples are now given to validate the theory and indicate its range of application. The first three examples compare results obtained by a number of authors for simply supported or cantilevered beams that have

been widely used as test examples. The fourth and fifth examples are used to validate the accuracy of the proposed theory when used to analyze structures formed from sandwich beams. The final example considers a simple frame for which the values of some of the natural frequencies can be argued through a self consistency check.

Table 1. sets out various groups of material and geometric properties that define the member(*s*) used in each of the examples.

Table 1
Details of the material and geometric properties of the members used in the numerical examples.

Propery group No.	$E_t = E_b$ GPa	E_c GPa	G_c MPa	$G_t = G_c$ MPa	$\rho_t = \rho_b$ kg/ m^3	ρ_c kg/ m^3	t_t mm	t_b mm	t_c mm
1	68.9	0	82.68	∞	2680	32.8	0.4572	0.4572	12.7
2	210	0.0015	0.3333	53333	7850	950	2	3	20
3	210	0	0.3333	∞	7850	950	2	3	20
4	210	16	3667	53333	7850	11100	2	3	20
5	210	0	3667	∞	7850	11100	2	3	20
6	69	0	440	∞	3180	83	0.56	0.56	25.4
7	69	0	440	2620	3180	83	0.56	0.56	25.4

E_t, E_b and E_c are the Young's moduli of the top, bottom and core layers, respectively, G_t, G_b and G_c are the shear modulus of the top, bottom and core layers, respectively, ρ_t, ρ_b and ρ_c are the densities of the top, bottom and core layers, respectively, and t_t, t_b and t_c are the thicknesses of the top, bottom and core layers, respectively.

Example 1: The first problem considers a sandwich beam whose properties are defined in Property Group 1 and which has length $0.9144m$, identical faceplates and the following boundary conditions, $W = M = N_b = N_t = 0$, at each end of the member. Such boundary conditions are correctly described as 'roller-roller' supports and are identical to the 'simple supports' described in those papers reporting comparative results in Table 2. However, the term 'simple support' needs to be clarified, since the position on the cross-section of the longitudinal constraint has a significant effect on the vibration of the beam. See the Appendix and reference [29]. Thus, when comparing the results in Table 2., it should be noted that those stemming from references [7,21,30] do not allow for coupled longitudinal inertia and those stemming from references [13,14] do not relate to an identically comparable set of field displacements.

Table 2
Comparative results for the non-zero natural frequencies (Hz) of the roller-roller§ supported sandwich beam of Example 1 using property group No. 1.

Freq. No.*	Mode+	Current theory	[21]	[7]	[30]	[14]	[13]
1	B1	57.1241	57.1358	56.159	57.5	57.068	57.041
2	B2	219.431	219.585	215.82	-	218.569	218.361
3	B3	464.595	465.172	457.22	467	460.925	460.754
4	B4	766.915	768.177	755.05	-	757.642	758.692
5	B5	1104.63	1106.68	1087.9	1111	1086.955	1097.055
6	B6	1462.31	1465.10	1440.3	-	1433.920	1457.064
7	B7	1830.14	1833.55	1802.7	1842	1789.345	1849.380
8	B8	2202.32	2206.19	2169.8	-	2147.969	2275.916
9	A1	2563.22	-	-	-	-	2562
10	B9	2575.62	2579.79	2538.2	2594	-	-
11	B10	2948.30	2952.65	2906.2	-	-	-
17	A2	5126.44	-	-	-	-	-
26	A3	7689.67	-	-	-	-	-
54	S1	16406.4	-	-	-	-	-
56	S2	16642.4	-	-	-	-	-

§ Except for the current theory, the term "simply supported" is used by others.
* 'Freq. No.' indicates the order of occurrence of the modes.
+ The predominant component of the mode and it's ordering number. For example, 'B1' indicates the first bending mode, 'A1', the first axial mode, 'S2', the second shear thickness mode and so on.

Example 2: The beam of Example 1 is now constrained to act as a cantilever and its length is reduced to $0.7112m$. Comparative results for the first eight natural frequencies are presented in Table 3.

Table 3
Comparative results for the natural frequencies (Hz) of a cantilevered sandwich beam of length $0.7112m$ with material properties given in Property Group No. 1.

Freq. No.*	Mode+	Proposed theory	[21]	[30]	[7]	[20]	[22]	[13]	
								HOBT4b	HOBT5
1	B1	33.7459	33.7513	33.97	33.146	31.46	33.74	33.7	33.7
2	B2	198.798	198.992	200.5	195.96	193.7	198.8	197.5	197.5
3	B3	511.420	512.307	517	503.43	529.2	511.4	505.5	505.5
4	B4	905.226	907.299	918	893.28	1006	905.1	890.5	890.5
5	B5	1346.23	1349.65	1368	1328.5	-		1321	1321
6	A1	1647.79	-	-	-	-		1648	1648
7	B6	1811.15	1815.82	1844	1790.7	-		1786	1786
8	B7	2286.77	2292.45	2331	2260.2	-		2271	2271
9	B8	2765.80	2772.23	2824	2738.9	-		2792	2792
14	A2	4943.36	-	-	-	-		4943§	4941§

*,+ See footnote of Table 2
§Reference [13] indicates that values correspond to the second axial mode but frequency no. 13.

Example 3: The third example is a cantilevered sandwich beam with unsymmetrical cross-section of length $0.5m$ for which the top and bottom layers have thicknesses $2mm$ and $3mm$ respectively and are made of steel. The middle core layer has thickness $20mm$ and possesses the two different material properties of rubber and lead in turn. The material properties are given in Table 1. in Property Groups 2 to 5. Property Groups 2 and 4 include appropriate values of E_c and G_c required by the more sophisticated model of reference [22], while Property Groups 3 and 5 give the corresponding data with the equivalent properties for E_c and G_c in the proposed model. Comparative results are given in Table 4. and show good agreement for the rubber core model, but less so for the unlikely lead core model in which the lead contributes significant bending stiffness that is not accounted for herein.

Table 4
Comparative results for the circular natural frequencies of the cantilever beam of Example 3.

Property Group No.	2	3	4	5
Freq.No.*	[22]	Proposed theory	[22]	Proposed theory
1	67.5	67.5	321.4	307.6
2	316.6	316.6	1864	1798.6
3	827.7	827.7	4718	4589.4
4	1594	1594.3	7193	6297.5

* See footnote of Table 2.

Example 4: A circularly curved sandwich beam that is fully clamped at both ends is now considered, see Fig. 8. The length of the curve is $0.7112m$ and its radius is $4.2672m$. Comparative results for the first five natural frequencies (Hz) of this beam are given in Table 5. In addition, Table 6. shows the results of modeling the beam with the proposed theory using different numbers of identical straight elements. From Table 6. it is clear that modeling the curved beam with 4 such elements gives acceptable accuracy in the results.

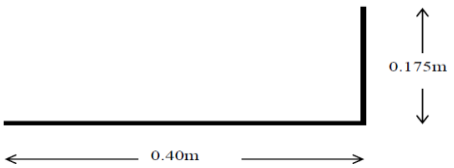

Fig.8
The free-free rigidly jointed frame of Example 5.

Example 5: Reference [34] considers the experimental evaluation and theoretical (FEM) verification of the natural frequencies of a uniform three-dimensional sandwich plate structure whose cross-section is identical to the L shaped frame of Fig. 9. The structure comprises two, rigidly jointed sandwich beams of length $0.175m$ and $0.4m$ with identical material and cross-sectional properties that correspond to Property Group No. 6. Our proposed model is able to replicate the fundamental bending mode of the original structure, comprising flexure of the two arms, but not the more complicated modes that involve torsional displacements along its length. Table 7. shows the first five, free-free natural frequencies of the frame in Fig. 8 according to the proposed theory, together with the comparison of the fundamental frequency of the original structure from reference [34].

Table 5
Comparative results for the first five natural frequencies (Hz) of the clamped-clamped curved sandwich beam of Example 4 using property group No. 1. §

Freq. No.*	Current theory	[30]	[31]	[32]	[33]	[35]	[18]
1	244.168	264	240	244.6	237.8	243.2431	263.094
2	484.384	522	474	485.6	504	477.4111	517.882
3	856.020	889	843	859.8	866	839.3961	875.794
4	1267.82	1312	1253	1276	1283	1237.50	1286.882
5	1710.42	1767	1697	1725	1728	1664.37	1728.185

* See footnote Table 2
§ The results in column 2 were obtained by modelling the structure with 10 straight elements. The results in columns three and four were obtained using 10 curved finite elements developed according to traditional assumptions.

Table 6
An assessment of the accuracy of the idealisation when modelling the curved sandwich beam of Example 4 with straight elements derived from the proposed theory for the first five natural frequencies (Hz).

Freq.No.*	Number of straight elements used to model the curve							
	2	3	4	5	6	8	10	20
1	236.885	241.914	243.148	243.626	243.860	244.075	244.168	244.284
2	485.212	484.522	484.478	484.440	484.418	484.395	484.384	484.369
3	861.824	854.552	855.101	855.540	855.748	855.938	856.020	856.123
4	1268.88	1268.07	1268.44	1268.01	1267.95	1267.86	1267.82	1267.76
5	1714.25	1716.34	1710.24	1710.47	1710.29	1710.39	1710.42	1710.46

* See footnote Table 2

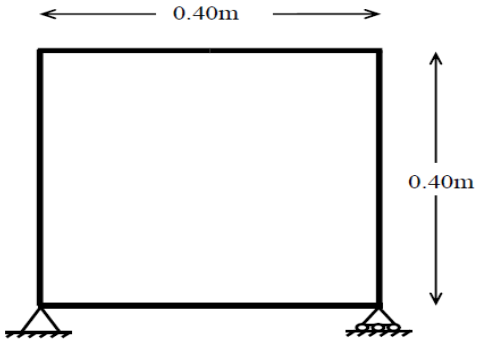

Fig.9
The pin-roller supported frame of Example 6.

Table 7
Results for the first five in-plane natural frequencies (Hz) of the free-free, *L*-shaped frame of Example 5 according to the proposed theory and a comparative value for the fundamental.

Property group No	6	7	
Freq.No.*	Current theory	[34]	
		Experimental	FEM
1	483.4	479.24	478
2	1031.4	-§	-
3	2284.6	-	-
4	3167.4	-	-
5	3959.1	-	-

* See footnote Table 2
§ The other four modes of vibration contain out of plane torsional deformation and therefore are not comparative.

Example 6: Fig. 10 shows a square, rigidly jointed plane frame constructed from four identical sandwich members. It is supported on pin-roller supports, where the horizontal constraint is imposed at the lower edge of the bottom faceplate of the bottom member. The length of each member is $0.40m$. Since the authors were unable to find any results in the literature for a comparable frame, the initial results for this frame were checked for consistency by increasing the axial rigidities by 10^3, a factor that is often used to make a structural element effectively in-extensible. On this assumption it is easy to argue that the fourth natural frequency of the frame will have a mode shape in which the moment contributed by each member at a joint balance to give zero rotation and must therefore correspond to the clamped ended natural frequency of an individual member. In this case the comparison will not be absolutely precise since the members are not completely in-extensible. The results are shown in Table 8.

Table 8
The first six natural frequencies (Hz) of the pin-roller supported frame of Example 6 for property group No. 1 and various axial rigidities of the faceplates. The clamped-ended frequency of a component member has been determined independently as $1794.927Hz$ and compares closely with the fourth frequency of the frame.

	Axial rigidity of each faceplate, $EA \times n$					
Freq. No.*	$n = 1$	$n = 5$	$n = 10$	$n = 50$	$n = 100$	$n = 1000$
1	120.5597	236.2467	294.1580	393.2158	414.1590	436.2600
2	449.3290	899.0634	1137.489	1577.231	1676.611	1784.083
3	656.9620	1158.450	1351.973	1632.770	1698.095	1784.598
4	750.7903	1328.063	1551.367	1744.639	1770.458	1794.660
5	884.3581	1413.161	1573.129	1879.365	1954.698	2053.488
6	1547.585	2664.531	3035.691	3456.595	3522.775	3587.312

* See footnote Table 2

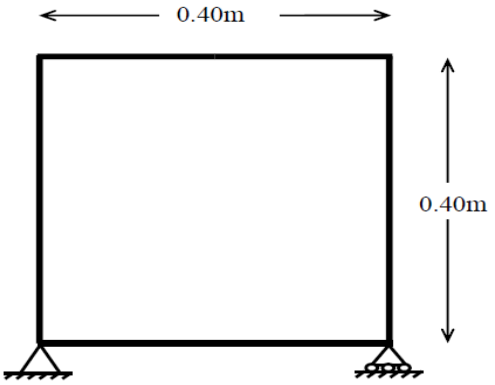

Fig.10
The pin-roller supported frame of Example 6.

6 GENERAL REMARKS

Sandwich beams have three fundamentally different types of mode of vibration; flexural, axial and shear thickness. A pure shear thickness mode is a mode in which the beam remains straight, without any lateral deflection or uniform extension in the usual sense. Instead, the faceplates displace horizontally relative to each other causing the core to deform in pure shear. The span length of the roller-roller supported beams does not affect the frequency of the fundamental shear thickness mode.

The three families of modes are normally coupled, but in some special cases it is possible to have uncoupled modes. For example, in a roller-roller supported sandwich beam with symmetric cross-section, the axial and flexural modes are uncoupled. Also the fundamental shear thickness mode is always a pure shear mode. Furthermore, a study of the mode shapes of the roller-roller beam shows that except for the fundamental shear thickness mode, the higher shear thickness modes always couple with flexural modes, with the result that two modes exist with the same number of half-waves in the transverse direction. The only difference between these two modes being an opposite sign associated with the average rotation of the cross-section and the general slope of the beam. A wider study shows that even for a completely symmetric beam, if the axial rigidity of the faceplates is increased, besides increasing the axial frequencies, the frequencies of the other families of modes are also increased. This means that the flexural and shear thickness modes are influenced by axial rigidity [29]. A further crucial point is to distinguish fully between sandwich beams and homogeneous beams, since the thickness in the former plays an important role in the behavior of the beam in the shear thickness mode of vibration and consequently on the coupling of the modes. In contrast with homogeneous beams, the position of the axial constraint through the thickness of the beam is important. This leads to variations in coupling between the modes, as well as differences in corresponding frequencies.

The use of the stiffness method offers great flexibility to analyze two dimensional structures, as well as to impose 'constraints' on any selected freedom of the structure. The latter will typically take the form of mass inertia, spring support stiffness or relationships that constrain one or more displacements to move in a predefined way relative to another set of displacements. Imposing such constraints follows the normal rules that would apply to a traditional beam element, except that more care is required to associate the constraint with the appropriate degree(s) of freedom. Also by using the appropriate transformations, as discussed in the Appendix, the developed element can be used to model structures constructed from sandwich beams. Example 5 shows good correlation between the present authors' results for the *L*-shaped frame and the experimental and FEM results of reference [34].

Furthermore, although the proposed element is straight, it can be used to model curved structures by using an appropriate number of straight elements to model the geometry of the curve. The results of Example 4 show that the number of straight elements needed is even less than the number of curved finite elements required to analyse a circularly curved arch. Ref. [31] compares the results of an FEM analysis with 6, 8 and 10 curved elements and shows that at least 10 elements are required for sufficient accuracy. However, Table 6. shows that the necessary convergence is achieved with only 4 of the proposed straight elements and the error with respect to the case with 10 such elements is less than 0.5 percent. Moreover, it should be noted that the results from reference [31] are always lower bounds, while those from [30] are always upper bounds, due to the different assumptions in each reference.

The results of Examples 1 to 5 show good correlation between the proposed theory and a selection of comparable results available in the literature. The differences in the results are attributable to many factors that vary widely from their approximate solution techniques to differences in basic assumptions. Also, the results of Example 6 provide a range of 'exact' solutions that may be helpful for future comparisons.

Finally, it is worth noting that while assembling the results it became apparent that it is relatively easy to generate an example in which the roots of the characteristic equation, Eq. (27), become sufficiently large that the value of ζ in Eq. (27b) overflows, even when using double precision arithmetic. However, because the combined effects of the roots and the length of the member are the source of this difficulty, reducing the length of the member (element) can help. Thus, if difficulty is experienced, a simple method is to subdivide the member into a greater number of elements until the problem is resolved.

7 CONCLUSIONS

A method for converging with certainty upon any required natural frequency of a rigid frame constructed from sandwich elements has been presented. It uses exact member theory in conjunction with the dynamic stiffness technique and this necessitates the solution of a transcendental eigenvalue problem. Solutions are achieved by use of the Wittrick-Williams algorithm, which yields the required natural frequencies to any desired accuracy in such a way that no difficulties are experienced with close or coincident natural frequencies or those exceptional natural frequencies which correspond to the nodal displacement vector being zero. The method therefore provides a very attractive alternative to the traditional finite element technique in which the accuracy is sensitive to the idealization.

The investigation shows that three families of modes; flexural, axial and shear thickness, are expected for any structure made from sandwich elements. These families are normally coupled, except for some special cases. However, the coupled mode can usually be identified as having a predominant component. On the other hand, the higher shear thickness modes always couple with flexural modes and result in two modes with the same number of half-waves in the transverse direction. The only difference between these two modes being an opposite sign associated with the average rotation of the cross-section and the general slope of the beam.

APPENDIX A

One of the most practical sets of axial constraint is perhaps the one that comprises the longitudinal displacements at the external fibers of the faceplates, i.e. u_1 and u_4 of Fig. 6. The necessary transformation between Eqs. (32) and the desired set of displacements and forces is

$$\mathbf{d}=\begin{bmatrix} W_1\\ \Psi_1\\ U_{t1}\\ U_{b1}\\ W_2\\ \Psi_2\\ U_{t2}\\ U_{b2}\end{bmatrix}=\mathbf{T}_1\begin{bmatrix} W_1\\ \Psi_1\\ U_{11}\\ U_{41}\\ W_2\\ \Psi_2\\ \mathrm{U}_{12}\\ U_{42}\end{bmatrix}=\mathbf{T}_1\hat{\mathbf{d}}_1 \quad ;\mathbf{p}=\begin{bmatrix} Q_1\\ M_1\\ N_{t1}\\ N_{b1}\\ Q_2\\ M_2\\ N_{t2}\\ N_{b2}\end{bmatrix}=\tilde{\mathbf{T}}_1\begin{bmatrix} Q_1\\ \tilde{M}_1\\ N_{11}\\ N_{41}\\ Q_2\\ \tilde{M}_2\\ N_{12}\\ N_{42}\end{bmatrix}=\tilde{\mathbf{T}}_1\hat{\mathbf{p}}_1 \tag{A.1}$$

where the transformation matrices are

$$\mathbf{T}_1=\begin{bmatrix} 1 & 0 & 0 & 0 & 0 & 0 & 0 & 0\\ 0 & 1 & 0 & 0 & 0 & 0 & 0 & 0\\ 0 & -t_t/2 & 1 & 0 & 0 & 0 & 0 & 0\\ 0 & t_b/2 & 0 & 1 & 0 & 0 & 0 & 0\\ 0 & 0 & 0 & 0 & 1 & 0 & 0 & 0\\ 0 & 0 & 0 & 0 & 0 & 1 & 0 & 0\\ 0 & 0 & 0 & 0 & 0 & -t_t/2 & 1 & 0\\ 0 & 0 & 0 & 0 & 0 & t_b/2 & 0 & 1\end{bmatrix} \quad \text{and} \quad \tilde{\mathbf{T}}_1=\begin{bmatrix} 1 & 0 & 0 & 0 & 0 & 0 & 0 & 0\\ 0 & 1 & t_t/2 & -t_b/2 & 0 & 0 & 0 & 0\\ 0 & 0 & 1 & 0 & 0 & 0 & 0 & 0\\ 0 & 0 & 0 & 1 & 0 & 0 & 0 & 0\\ 0 & 0 & 0 & 0 & 1 & 0 & 0 & 0\\ 0 & 0 & 0 & 0 & 0 & 1 & t_t/2 & -t_b/2\\ 0 & 0 & 0 & 0 & 0 & 0 & 1 & 0\\ 0 & 0 & 0 & 0 & 0 & 0 & 0 & 1\end{bmatrix} \tag{A.2}$$

The transformed dynamic stiffness matrix, $\hat{\mathbf{k}}_1$, follows through the following steps

$$\tilde{\mathbf{T}}_1\hat{\mathbf{p}}_1=\mathbf{k}\mathbf{T}_1\hat{\mathbf{d}}_1 \;;\quad \hat{\mathbf{p}}_1=\tilde{\mathbf{T}}_1^{-1}\mathbf{k}\mathbf{T}_1\hat{\mathbf{d}}_1 \;;\quad \hat{\mathbf{p}}_1=\hat{\mathbf{k}}_1\hat{\mathbf{d}}_1 \;;\quad \hat{\mathbf{k}}_1=\tilde{\mathbf{T}}_1^{-1}\mathbf{k}\mathbf{T}_1 \tag{A.3}$$

From Eq. (A.2) it can be deduced that $\tilde{\mathbf{T}}_1^{-1} = \mathbf{T}_1^{\mathrm{T}}$, where superscript *T* denotes the transpose of the matrix, and therefore

$$\hat{\mathbf{k}}_1 = \mathbf{T}_1^{\mathrm{T}} \mathbf{k}\, \mathbf{T}_1 \tag{A.4}$$

In the case where the core/faceplate interfaces are chosen as the axial freedoms, i.e. u_2 and u_3 in Fig. 6, it is only necessary to change the sign of all of the non-diagonal elements of the transformation matrices of Eq. (A.2).

Another useful transformation enables the average axial displacement of the face layers, u , to be used, thus requiring only one axial displacement at each end of the beam. However, its vertical position across the beam thickness is not fixed and varies due to changes in the values of u_t and u_b . The average rotation of the beam cross-section, φ , is the by-product of this transformation. From Fig. 6, it is clear that

$$u = \frac{u_t + u_b}{2} \quad and \quad \varphi = \frac{u_t - u_b}{d} \tag{A.5}$$

Consequently, the resultant axial force in the beam's cross-section, n , and the couple due to the axial forces developed in the top and bottom faceplates during bending, $\bar{\mathrm{m}}$, become

$$n = n_t + n_b \quad and \quad \bar{\mathrm{m}} = n_t \frac{d}{2} - n_b \frac{d}{2} = (n_t - n_b)\frac{d}{2} \tag{A.6}$$

with regard to Eq. (32), the necessary transformations between the displacements and forces can be written as:

$$\mathbf{d} = \begin{bmatrix} W_1 \\ \Psi_1 \\ U_{t1} \\ U_{b1} \\ W_2 \\ \Psi_2 \\ U_{t2} \\ U_{b2} \end{bmatrix} = \mathbf{T}_2 \begin{bmatrix} W_1 \\ \Psi_1 \\ \Phi_1 \\ U_1 \\ W_2 \\ \Psi_2 \\ \Phi_2 \\ U_2 \end{bmatrix} = \mathbf{T}_2 \hat{\mathbf{d}}_2 \quad ; \quad \mathbf{p} = \begin{bmatrix} Q_1 \\ M_1 \\ N_{t1} \\ N_{b1} \\ Q_2 \\ M_2 \\ N_{t2} \\ N_{b2} \end{bmatrix} = \tilde{\mathbf{T}}_2 \begin{bmatrix} Q_1 \\ M_1 \\ \bar{M}_1 \\ N_1 \\ Q_2 \\ M_2 \\ \bar{M}_2 \\ N_2 \end{bmatrix} = \tilde{\mathbf{T}}_2 \hat{\mathbf{p}}_2 \tag{A.7}$$

where the transformation matrices are

$$\mathbf{T}_2 = \begin{bmatrix} 1 & 0 & 0 & 0 & 0 & 0 & 0 & 0 \\ 0 & 1 & 0 & 0 & 0 & 0 & 0 & 0 \\ 0 & 0 & d/2 & 1 & 0 & 0 & 0 & 0 \\ 0 & 0 & -d/2 & 1 & 0 & 0 & 0 & 0 \\ 0 & 0 & 0 & 0 & 1 & 0 & 0 & 0 \\ 0 & 0 & 0 & 0 & 0 & 1 & 0 & 0 \\ 0 & 0 & 0 & 0 & 0 & 0 & d/2 & 1 \\ 0 & 0 & 0 & 0 & 0 & 0 & -d/2 & 1 \end{bmatrix} \; ; \; \tilde{\mathbf{T}}_2 = \begin{bmatrix} 1 & 0 & 0 & 0 & 0 & 0 & 0 & 0 \\ 0 & 1 & 0 & 0 & 0 & 0 & 0 & 0 \\ 0 & 0 & 1/d & 1/2 & 0 & 0 & 0 & 0 \\ 0 & 0 & -1/d & 1/2 & 0 & 0 & 0 & 0 \\ 0 & 0 & 0 & 0 & 1 & 0 & 0 & 0 \\ 0 & 0 & 0 & 0 & 0 & 1 & 0 & 0 \\ 0 & 0 & 0 & 0 & 0 & 0 & 1/d & 1/2 \\ 0 & 0 & 0 & 0 & 0 & 0 & -1/d & 1/2 \end{bmatrix} \tag{A.8}$$

In similar fashion to Eq.(A.3), the new transformed stiffness matrix is

$$\hat{\mathbf{k}}_2 = \mathbf{T}_2^{\mathrm{T}} \mathbf{k}\, \mathbf{T}_2 \tag{A.9}$$

Finally, to include a beam in a plane frame, it is necessary to transform the stiffness matrix from member co-ordinates to global co-ordinates (see Fig. 7). During transformation the rotations and moments remain unchanged. Thus from Fig. 7 it is clear that

$$\begin{cases} X = W\sin\theta + U\cos\theta \\ Y = W\cos\theta - U\sin\theta \end{cases} \qquad \begin{cases} P_x = Q\sin\theta + N\cos\theta \\ P_y = Q\cos\theta - N\sin\theta \end{cases} \tag{A.10}$$

The transformations can then be written in matrix notation as:

$$\hat{\mathbf{d}}_2 = \begin{bmatrix} W_1 \\ \Psi_1 \\ \Phi_1 \\ U_1 \\ W_2 \\ \Psi_2 \\ \Phi_2 \\ U_2 \end{bmatrix} = \mathbf{T}_3 \begin{bmatrix} X_1 \\ Y_1 \\ \Psi_1 \\ \Phi_1 \\ X_2 \\ Y_2 \\ \Psi_2 \\ \Phi_2 \end{bmatrix} = \mathbf{T}_3 \mathbf{d}_G \quad ; \quad \hat{\mathbf{p}}_2 = \begin{bmatrix} Q_1 \\ M_1 \\ \bar{M}_1 \\ N_1 \\ Q_2 \\ M_2 \\ \bar{M}_2 \\ N_2 \end{bmatrix} = \mathbf{T}_3 \begin{bmatrix} P_{x1} \\ P_{y1} \\ M_1 \\ \bar{M}_1 \\ P_{x2} \\ P_{y2} \\ M_2 \\ \bar{M}_2 \end{bmatrix} = \mathbf{T}_3 \mathbf{p}_G \tag{A.11}$$

where subscript *G* denotes quantities in global co-ordinates and the transformation matrix is

$$\mathbf{T}_3 = \begin{bmatrix} \sin\theta & \cos\theta & 0 & 0 & 0 & 0 & 0 & 0 \\ 0 & 0 & 1 & 0 & 0 & 0 & 0 & 0 \\ 0 & 0 & 0 & 1 & 0 & 0 & 0 & 0 \\ \cos\theta & -\sin\theta & 0 & 0 & 0 & 0 & 0 & 0 \\ 0 & 0 & 0 & 0 & \sin\theta & \cos\theta & 0 & 0 \\ 0 & 0 & 0 & 0 & 0 & 0 & 1 & 0 \\ 0 & 0 & 0 & 0 & 0 & 0 & 0 & 1 \\ 0 & 0 & 0 & 0 & \cos\theta & -\sin\theta & 0 & 0 \end{bmatrix} \tag{A.12}$$

Hence, the element stiffness matrix in global co-ordinates, $\mathbf{k}_G$, is

$$\mathbf{k}_G = \mathbf{T}_3^{\mathrm{T}} \hat{\mathbf{k}}_2\, \mathbf{T}_3 = \mathbf{T}_3^{\mathrm{T}} \mathbf{T}_2^{\mathrm{T}} \mathbf{k}\, \mathbf{T}_2 \mathbf{T}_3 \tag{A.13}$$

REFERENCES

[1] Kerwin E. M., 1959, Damping of flexural waves by a constrained viscoelastic layer, *Journal of the Acoustical Society of America* **31**: 952-962.

[2] Mead D. J., 1962, *The Double-Skin Damping Configuration*, University of Southampton.

[3] DiTaranto R. A., 1965, Theory of vibratory bending for elastic and viscoelastic layered finite-length beams, *Journal of Applied Mechanics* **32**: 881-886.

[4] Yin T. P., Kelly T. J., Barry J. E., 1967, A quantitative evaluation of constrained layer damping, *Transactions of the American Society of Mechanical Engineers, Journal of Engineering for Industry* **89**: 773-784.

[5] Mead D. J., Markus S., 1969, The forced vibration of a three-layer, damped sandwich beam with arbitrary boundary conditions, *Journal of Sound and Vibration* **10**: 163-175.

[6] Rao D. K., 1978, Frequency and loss factors of sandwich beams under various boundary conditions, *Journal of Mechanical Engineering Science* **20**: 271-282.

[7] Sakiyama T., Matsuda H., Morita C., 1996, Free vibration analysis of sandwich beam with elastic or viscoelastic core by applying the discrete Green function, *Journal of Sound and Vibration* **191**: 189-206.

[8] Yu Y.Y., 1959, A new theory of elastic sandwich plate-one dimensional case, *Journal of Applied Mechanics* **26**: 415-421.

[9] Rao Y. V. K. S., Nakra B. C., 1970, Influence of rotary and longitudinal translatory inertia on the vibrations of unsymmetrical sandwich beams, *Proceeding of the 15th Conference I.S.T.A.M.*

[10] Mead D. J., 1982, A comparison of some equations for the flexural vibration of damped sandwich beams, *Journal of Sound and Vibration* **83**: 363-377.

[11] Chonan S., 1982, Vibration and stability of sandwich beams with elastic bonding, *Journal of Sound and Vibration* **85**(4): 525-537.

[12] Mead D. J., Markus S., 1985, Coupled flexural, longitudinal and shear wave motion in two- and three-layered damped beams, *Journal of Sound and Vibration* **99**(4): 501-519.

[13] Marur S. R., Kant T., 1996, Free vibration analysis of fiber reinforced composite beams using higher order theories and finite element modeling, *Journal of Sound and Vibration* **194**: 337-351.

[14] Kameswara Rao M., Desai Y.M., Chitnis M. R., 2001, Free vibration of laminated beams using mixed theory, *Composite Structures* **52**: 149-160.

[15] Silverman I. K., 1995, Natural frequencies of sandwich beams including shear and rotary effects, *Journal of Sound and Vibration* **183**: 547-561.

[16] Fasana A., Marchesiello S., 2001, Rayleigh-Ritz analysis of sandwich beams, *Journal of Sound and Vibration* **241**: 643-652.

[17] Amirani M. C., Khalili S. M. R., Nemati N., 2009, Free vibration analysis of sandwich beam with FG core using the element free Galerkin method, *Composite Structures* **90**: 373-379.

[18] Hashemi S. M., Adique E. J., 2009, Free vibration analysis of sandwich beams: A dynamic finite element, *International Journal of Vehicle Structures and Systems* **1**(4): 59-65.

[19] Hashemi S. M., Adique E. J., 2010, A quasi-exact dynamic finite element for free vibration analysis of sandwich beams, *Applied Composite Materials* **17**(2): 259-269.

[20] Banerjee J. R., 2003, Free vibration of sandwich beams using the dynamic stiffness method, *Computers and Structures* **81**: 1915-1922.

[21] Howson W. P., Zare A., 2005, Exact dynamic stiffness matrix for flexural vibration of three-layered sandwich beams, *Journal of Sound and Vibration* **282**: 753-767.

[22] Banerjee J. R., Sobey A.J., 2005, Dynamic stiffness formulation and free vibration analysis of a three-layered sandwich beam, *International Journal of Solids and Structures* **42**(8): 2181-2197.

[23] Banerjee J. R., Cheung C. W., Morishima R., Perera M., Njuguna J., 2007, Free vibration of a three-layered sandwich beam using the dynamic stiffness method and experiment, *International Journal of Solids and Structures* **44**: 7543-7563.

[24] Jun L., Xiaobin L., Hongxing H., 2009, Free vibration analysis of third-order shear deformable composite beams using dynamic stiffness method, *Archive of Applied Mechanics* **79**: 1083-1098.

[25] Khalili S. M. R., Nemati N., Malekzadeh K., Damanpack A. R., 2010, Free vibration analysis of sandwich beams using improved dynamic stiffness method, *Composite Structures* **92**: 387-394.

[26] Damanpack A. R., Khalili S. M. R., 2012, High-order free vibration analysis of sandwich beams with a flexible core using dynamic stiffness method, *Composite Structures* **94**: 1503-1514.

[27] Wittrick W. H., Williams F. W., 1971, A general algorithm for computing natural frequencies of elastic structures, *Quarterly Journal of Mechanics and Applied Mathematics* **24**: 263-284.

[28] Howson W. P., Williams F. W., 1973, Natural frequencies of frames with axially loaded Timoshenko members, *Journal of Sound and Vibration* **26**: 503-515.

[29] Zare A., 2004, *Exact Vibrational Analysis of Prismatic Plate and Sandwich Structures*, Ph.D. Thesis, Cardiff University.

[30] Ahmed K. M., 1971, Free vibration of curved sandwich beams by the method of finite elements, *Journal of Sound and Vibration* **18**: 61-74.

[31] Ahmed K. M., 1972, Dynamic analysis of sandwich beams, *Journal of Sound and Vibration* **10**: 263-276.

[32] Sakiyama T., Matsuda H., Morita C., 1997, Free vibration analysis of sandwich arches with elastic or viscoelastic core and various kinds of axis-shape and boundary conditions, *Journal of Sound and Vibration* **203**(3): 505-522.

[33] Bozhevolnaya E., Sun J. Q., 2004, Free vibration analysis of curved sandwich beams, *Journal of Sandwich Structures & Materials* **6**(1): 47-73.

[34] Petrone F., Garesci F., Lacagnina M., Sinatra R., 1999, Dynamical joints influence of sandwich plates, *Proceedings of the 3rd European Nonlinear Oscillations Conference*, Copenhagen, Denmark.

[35] Marura S. R., Kant T., 2008, Free vibration of higher-order sandwich and composite arches, Part I: Formulation, *Journal of Sound and Vibration* **310**: 91-109.